EVS27
Barcelona, Spain, November 17-20, 2013

Validation of the methodology for lithium-ion batteries lifetime prognosis

E. Sarasketa-Zabala*, I. Laresgoiti, I. Alava, M. Rivas, I. Villarreal, F. Blanco

IK4-Ikerlan, Energy Business Unit, Arabako Teknologi Parkea, Juan de La Cierva 1, E-01510 Miñao, Spain

**E-mail: esarasketa@ikerlan.es*

Abstract

Battery lifetime prognosis is a key requirement for successful market introduction of rechargeable Energy Storage Systems (ESS) based on lithium-ion (Li-ion) technology. In order to make decisions at the system design stage, a procedure for making efficient predictions of battery performance over time is necessary to be developed.

In this paper, a general methodology for the evaluation of lifetime prediction is presented, covering the semi-empirical aging model precision and validity. Both calendar-life and cycle-life performance were investigated. Moreover, standing time and working operation were examined jointly using realistic operating profiles. The aim was the predictive model to be suitable for any application, including electric vehicle (EV), within the considered operating range. The efforts were especially focused on model ratification procedures and predictions goodness evaluation. The validation processes not only dealt with static impact factors evaluation but also with dynamic operation schemes. Besides, integration of ageing monitoring algorithm into Battery Management System (BMS) was evaluated. Battery pack design and operation strategies definition criteria were also discussed based on the stress factors influence on cell performance. The presented results correspond to a lithium iron phosphate (LFP) cathode 26650-size Li-ion cell.

Keywords: Lithium-ion (Li-ion), lifetime prognosis, calendar life, cycle life, ageing model, State of Health (SOH)

1 Introduction

Li-ion batteries are the leading candidate for EV and other transportation applications due to specially their high energy and power density. Ageing at cell level is one of the key issues for this technology based ESS improvement, as long lifespan is required for target applications (e.g. 10 years for EV). It is therefore necessary establishing concise algorithms for long-term lifetime performance predictions based on short-term cell accelerated test data [1], as real operation condition tests are highly time and cost intensive. This research work aims to present an innovative methodology for the development of ageing models that simulate jointly cells standing time and working operation. The defined protocol pursues to come up with a compromise between the accuracy of the models and the experimental work to be carried out, focusing particularly in model ratification procedures. Not only are they based on additional tests under constant stress

conditions but also at dynamic operation schemes [2][3], as models needs to be extrapolated to any arbitrary real profile. So far, most of the ageing model validations are based on static impact factors evaluation [4][5]. Besides, reliable predictions needs of physical evidence so that degradation modes and cell performance are related over time, modelling this way ageing phenomena as accurate as possible. Additionally, taking into account the model precision according to the validation results, potential applications of the obtained lifetime prognosis mathematical models are to be discussed.

The reference selected for the reported study was a commercially available $LiFeOP_4$ (LFP)/graphite 26650-size cell with 2.3Ah nominal capacity. Olivine-type lithium phosphate is one of the cathode materials of main interest for EV applications because of its safe performance, low cost, high specific power and high cycling capability. When it comes to the cell configuration, cylindrical casing is one of the most widely used packaging styles.

2 Lifetime prognosis methodology

Fig. 1 depicts the approach followed for ageing model development. The causes affecting ageing (stress or impact factors) and the measurement of their contribution to cell performance over time (ageing metrics) are outlined in Fig. 2. Influence of current rate (C-rate), State of Charge (SOC), Depth of Discharge (DOD) and temperature (T) in cell available capacity loss (C_{loss}) and internal resistance (IR) increase, meaning loss in dynamic current capability (i.e. power fade) and relaxation ability, are necessary to simulate in order to control the battery operation and thus the costs (effective ageing). Overall, the process for batteries lifetime optimisation is: (i) investigation of the battery stress factors, (ii) battery ageing model building, (iii) validation of the ageing model and, lastly, (iv) the implementation of the model to meet the pursued goal (e.g. battery pack sizing, Total Costs of Ownership (TCO) estimation, integration of the ageing model in BMS together with the electrical and thermal performance models, etc).

2.1 Experimental procedures

Extended accelerated ageing tests were performed under static conditions. Key calendar and cyclic ageing impact factors were separated in order to parameterise derived single semi-empirical relationships. Calendar ageing (A_{cal}) tests were carried out at different temperatures and SOCs at open circuit (OC), considering that self-discharge is of minor importance below 100% SOC [6]. On the other hand, symmetric charge sustaining cycling performance (A_{cyc}) was analysed as a

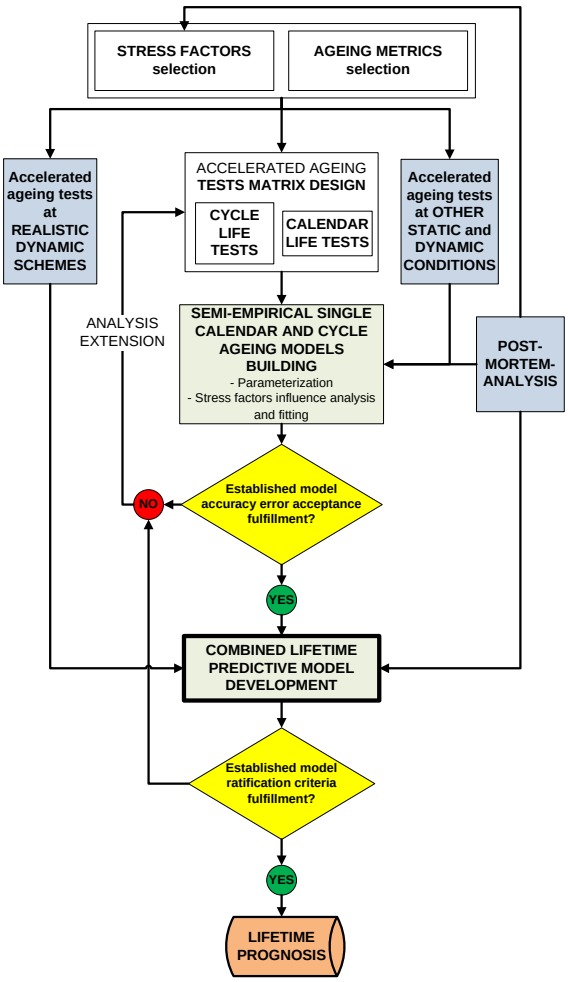

Figure 1: Methodology for lifetime prognosis (ratification procedures in blue)

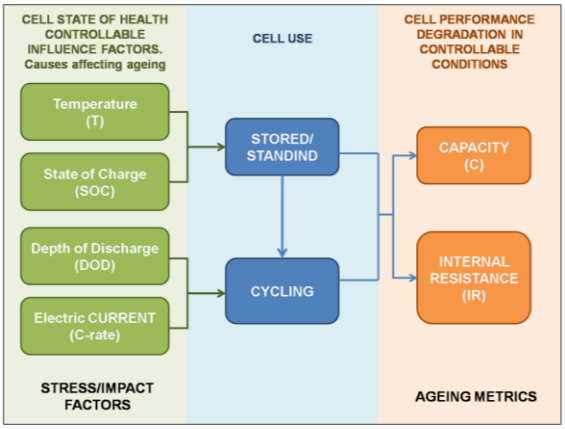

Figure 2: Controllable factors inducing changes in cell performance (both while working operation and standing time) when it comes to the battery's capacity and internal resistance

function of C-rates and DOD in accordance with the assumption made by other authors [7] [8] [9] that storage and cyclic ageing effects can be superimposed. That is to say:

$$A_{cal} = f(SOC, T, t) \quad (1)$$
$$A_{cyc} = f(DOD, C\text{-}rate, Ah\text{-}throughput) \quad (2)$$
$$A_{TOTAL} = A_{cal} + A_{cyc} = f(SOC, T, t, DOD, C\text{-}rate, Ah) \quad (3)$$

Apart from the factors that are under investigation in this paper, there are also other ones that contribute to the experiments. These may be gathered together into three main groups [10]: (i) uncontrollable factors such as cells variability, measurement error or ambient conditions (meaning humidity, pressure, etc.); (ii) nuisance factors, for instance Electrical Parameters Identification Tests (EPIT) schedule or cycling protocols change due to cell ageing; and (iii) factors that are considered constant: homogeneous temperature along the whole jelly-roll, conditioning procedure and so on. All these factors effect ought to be determined in order to assign an error to the precision of the predictions and extrapolations to the desired End of Life (EOL). Among others, cell-to-cell variations is an important factor, as single-cell experiments can strongly depend on the tested cell (i.e. influence on mean cell lifetime limits). This way, all the tests were run using cells of the same manufacturing batch which nominal capacity at the Beginning of Life (BOL) was 2.301±0.01Ah (95% confidence interval).

On the other hand, experiments were carried out correcting set parameters values (SOC and DOD) according to cell's actual capacity. In case the tests are done using always the same values, additional polarisation effects induced by a possible loss of active material show up in the data [11].

Evolution of cell's capacity and internal resistance were monitored for battery ageing model parameterisation by conducting the following intermittent EPIT at at room temperature (298K): (i) full charge-discharge cycles at nominal conditions (actual nominal capacity measurement), (ii) current pulses at cells maximum acceptable charge/discharge current rates over cell's entire SOC range (actual IR measurement), (iii) Electrochemical Impedance Spectroscopy (EIS) measurements (impedance change evaluation) and (iv) cell full discharge at very low C-rate (quasi-Open Circuit Voltage (OCV) curves examination). Cell voltage responses progress was analysed in order to understand cell behaviour and degradation. Incremental Capacity (IC) and Differential Voltage (DV) curves are key tools for diagnostics (e.g. cell impedance changes and loss of both active material and cyclable lithium identifications). These Reference Performance Tests (RPT) were carefully planned so that their impact on cell degradation was as negligible as possible.

In the present work, the EOL was defined to be reached when actual nominal capacity and IR were 80% and 200%, respectively, when normalised to initial values (i.e. increase of initial IR by a factor of 2). These limits were established in agreement with the most extended lifetime criteria for EVs.

2.2 Accelerated ageing tests

Many single-factorial variation experiments were carried out actively testing the external influence factors, which range limits were chosen within the cell operation window set by the manufacturer and taking also into account the cell behaviour observed during several screening initial tests. Nonetheless, temperature, SOC and C-rate outer limits were not checked since a real-life application may not work on them. Furthermore, effects of SOC and T as well as C-rate and DOD binary combinations were analysed at certain chosen levels.

Table 1 shows the static accelerated ageing tests bench matrix that was planned according to the assumptions already mentioned (note that the defined static validation tests are also included on it). All the cycling tests were performed at 303K and 50% mean SOC (baseline temperature and voltage cycling conditions).

Table 1: Test matrix for calendar and cyclic ageing models building and static validation (green ticks).

FACTORS	*Levels*	30% SOC	70% SOC	90% SOC		
SOC & T	303K		X			
	313K	X	X	X		
	323K		X	✓		
	Levels	5% DOD	10% DOD	30% DOD	60% DOD	100% DOD
C-rate & DOD	1C	X	X	✓	X	X
	2C				X	
	3.5C		X		X	

NOTE: Cycling was always conducted at 303K and 50% mean SOC

2.3 Ageing modelling

Ageing model was developed using a stress factors time-domain characterisation method, by capturing the dominant effects on cell performance degradation for fitting each single testing parameter. Fig. 4 depicts the approach followed for cell ageing prediction. This method uses and combines all possible key stress factors and provides cell State of Health (SOH) estimations beyond measured and simulated operating range and time.

2.4 Model validation protocols

Remarkable model ratification procedures (see Fig. 1) are additional accelerated tests at other static conditions, as indicated in Table 1 with green ticks, and also under dynamic ambient temperature, cycling current profile or even storing voltage bands, as depicted in Fig. 3. Moreover, cycling performance needs to be checked further so as to confirm the premise that the effect of SOC and temperature stress factors is the same during storage and operation.

It is also essential to understand ageing modes in order to establish a clear evolution of battery life. That is to say, to identify temporal correlation between performance fade and degradation mechanisms in order to verify, by means of physical evidence, the long-term lifetime prediction algorithms that are to be established based on short-term cell test data.

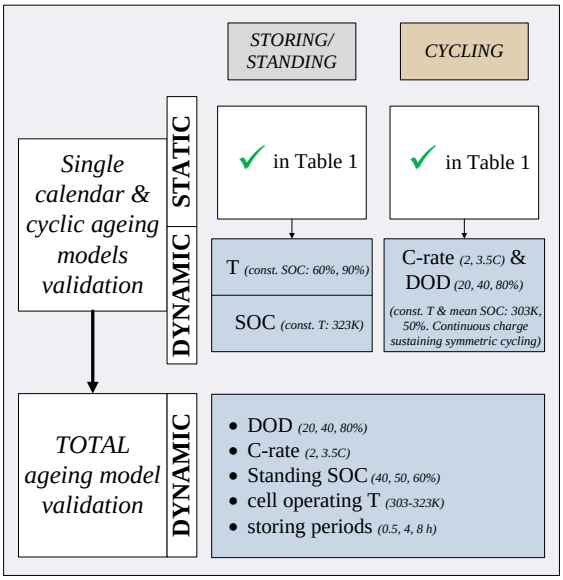

Figure 3: Validation tests

3 Results and discussions

In this section, results from accelerated ageing tests and modelling are presented together. Emphasis is set to describe the guidelines followed for the development of the models and the resulting lifetime predictions main issues.

3.1 Model development

Fig. 5, Fig. 6 and Fig. 7 show the experimental results of the evaluated ageing metrics together with the predictions, which correspond with

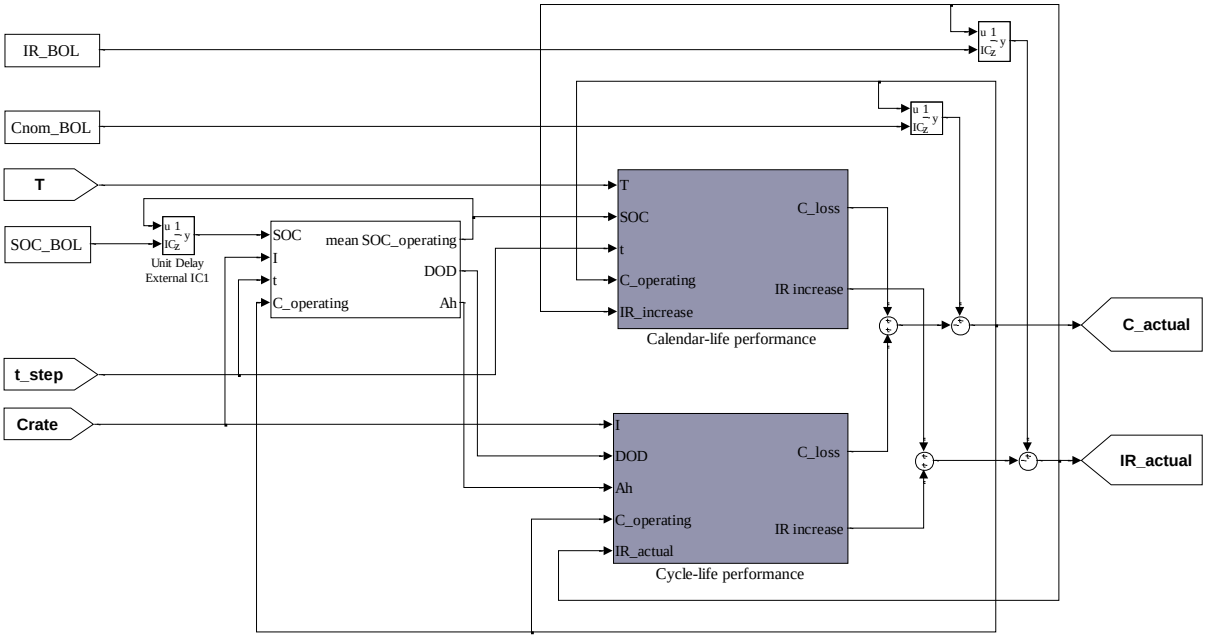

Figure 4: Ageing model. Available capacity and resistance offset prediction in response to time and controllable environmental influences (IR: Internal Resistance; C: Capacity; Cnom: Nominal capacity)

$$IR_{increase} = 1.29 \cdot 10^{11} \cdot exp(-9194/T) \cdot t \quad (4)$$

$$C_{loss\_cal} = 165400 \cdot exp(-4148/T) \cdot exp(0.01 \cdot SOC) \cdot t^{0.5} \quad (5)$$

$$C_{loss\_cyc} = (-0.14 - 0.08 \cdot DOD + 1.92 \cdot DOD^{0.5} - 2.51 \cdot ln(DOD)) \cdot (0.48 \cdot Crate^2 - 2.42 \cdot Crate + 1.57) \cdot t^{0.8} \quad (6)$$

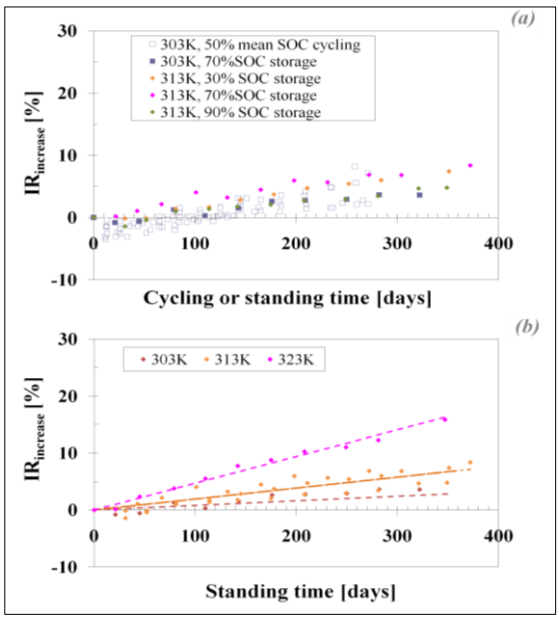

Figure 5: IR increase over time *(a)* during different cell operating conditions (cycling tests at different DOD and C-rates) and *(b)* as a function of temperature together with the developed model (Eq. (4)) simulations in dotted lines

Eq. (4), Eq. (5) and Eq. (6) according to the best fitting results (0.904, 0.987 and 0.912 adjusted coefficient of determinations, respectively).

EPIT demonstrated that the investigated LFP cell was aged primarily due to capacity fade rather than resistance increase as also reported by other authors [12] [13] [14]. An IR increase of just *ca.* 15% was measured after 350 days at most demanding conditions. Besides, it bears mentioning that an unexpected slight initial diminution of IR (*ca.* 3%) was observed, in agreement with other studies with the same cell configuration [13] [14]. The impact of SOC, T, DOD and C-rate on cell internal resistance is analysed in Fig. 5, which represents the IR measured using a discharge pulse at 50% SOC. Regardless of this metric testing procedure, i.e. charge or discharge current step and reference voltage (Fig. 8 and Fig. 9, respectively), the measured trend was similar, which simplifies meaningfully the prediction models. Fig. 5 *(a)* shows that there is no dependency between IR and either SOC or DOD, and even C-rate. On the one

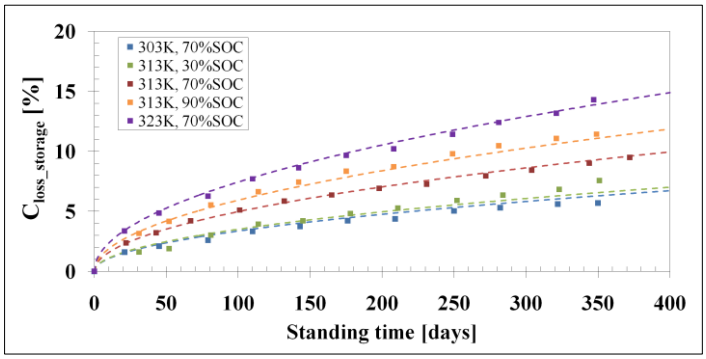

Figure 6: Capacity loss during storage at different temperatures and SOCs. Test data and built model (Eq. (5)) results in dotted lines

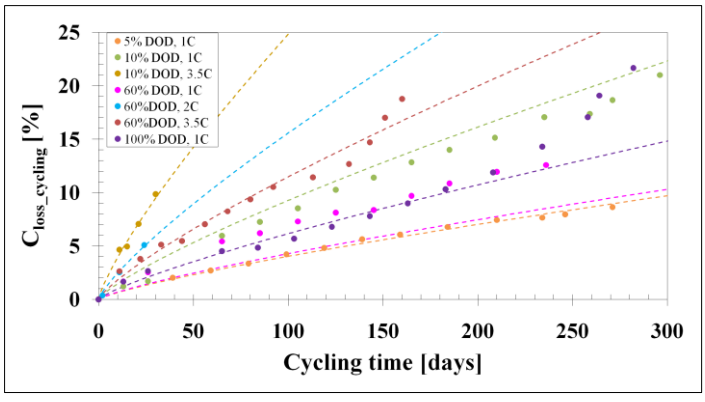

Figure 7: Continuous cycling time dependant capacity loss as a function of DOD and C-rate (303K, 50% mean SOC) over time. Experimental data and developed model (Eq. (6)) results in dotted lines

hand, it was observed that the induced IR change during cell cycling (at any condition) and storage was apparently similar for the same operating temperature. It was therefore assumed that cycling does not accelerate this ageing metric change. On the other hand, calendar ageing experimental results indicated that the effect of standing SOC on IR increase was not assessable. Thus, it was just modelled the influence of temperature and standing time on IR increase (Eq. (4)), as plotted in Fig. 5 *(b)* (note that experimental data at 313K correspond to cells stored at different SOC).

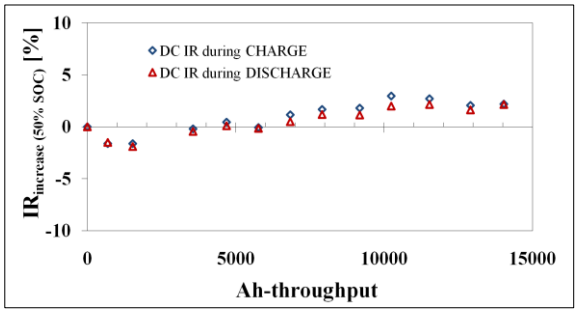

Figure 8: Current pulse EPIT results. DC Internal Resistance during charge and discharge at 50% SOC (cycling at 1C, 60% DOD, 50% mean SOC and 303K)

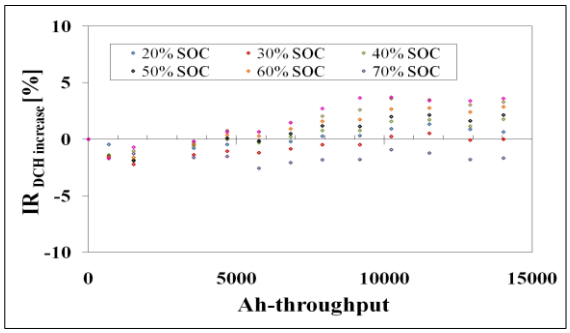

Figure 9: Current pulse EPIT results. DC Internal Resistance during discharge as a function of current pulse applying cell's SOC (cycling at 1C, 60% DOD, 50% mean SOC and 303K)

When it comes to the capacity loss, the effects of T, SOC and standing time are plotted in Fig. 6. On the one hand, parasitic chemical reactions followed an exponential relationship with temperature according to Arrhenius law. The measured activation energy was 34.5±14.9kJ/mol (95% Confidence Interval), which corresponds with that reported by other authors [14] for the same cell configuration. Regarding voltage impact on cell's capacity loss, which depends on cell cathode material, both linear [15] and exponential [16] evolutions were checked, being the latter the best fitting in all cases. Additionally, square root of time dependency was observed due to storage, which may be related to Solid Electrolyte Interface (SEI) layer increase over time as is typical for the cells containing carbon anode [17]. Overall, calendar ageing degradation modes may not change within the studied storing time frame (*ca.* a year) since the capacity loss evolution is stable over time (the error of the predictive model built after *ca*. 200 days of storing was reduced in a 0.32% when updating it after *ca.* a year, being at this time 0.99% the largest measured error).

Accounting for capacity offset during cycling, the influence of DOD, C-rate and the amount of charge through the battery are evaluated in Fig. 7. The level of stress was, as expected, increased ($t^{0.8}$) due to Ah-throughput. The results also indicate that there was little effect of cycling amplitude (DOD) on cell degradation rate, just like other authors also reported [18]. According to the developed predictive model, except for the specimens cycled at studied range limits (5% and 100% DOD), the 20% capacity fade was reached more or less after the same total Ah-throughput regardless the DOD. Hence, the effect of cycling time (or Ah-throughput) was more significant than DOD. The degradation rate was slowed-down at low DOD (tests at 5% DOD are still ongoing so as to analyse this phenomenon more in depth). On the contrary, when cell cycling at the largest voltage range, i.e. 100% DOD, the capacity loss process was sped up appreciably after *ca.* 12500 Ah through the battery, which may indicate that the induced possible degradation modes change over time. Loss of Lithium Inventory (LLI) was identified to be apparently the only degradation mode at any

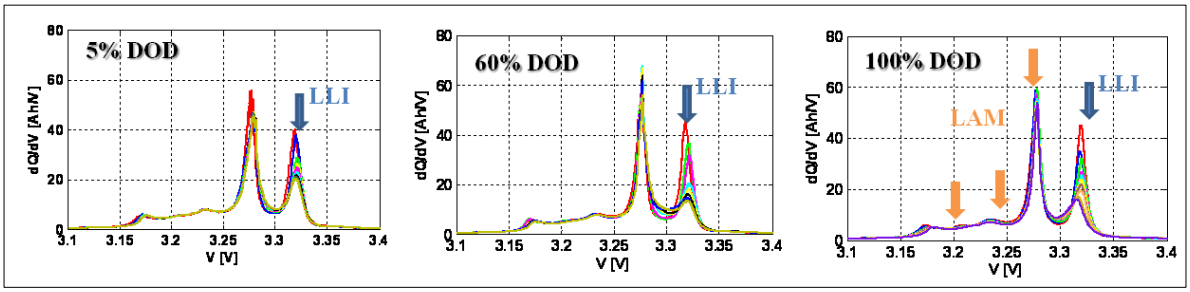

Figure 10: Differential Voltage (DV) signatures from the initial state (in red) to *ca.* 13800 Ah-throughput

studied DOD but for 100% DOD when IC and DV curves (Fig. 10) were analysed. At 100% DOD, however, Loss of Active Material (LLA) was additionally revealed. Post-mortem analysis is being conducted in order to understand the influence of DOD and detected possible degradation modes change at 100% DOD. When analysing C-rate effect, comparing the results of the tests at 3.5 and 1C (both at 60% DOD), it was observed that the standing time induces more the capacity loss than the operating electric current [19]. Besides, not only seems not to be larger the degradation at larger C-rates, but there are complex non-linear combined effects of DOD and C-rate. Tests at 2C (60% DOD) indicate that the operating current effect can be simulated using polynomial mathematical relationships (i.e. the degradation rate was enhanced at the studied intermediate C-rate). Moreover, in case the cell was cycled at other DOD, even if it was smaller, e.g. 10% DOD and 3.5C, the capacity loss was larger. More data is however required to fully understand all these phenomena.

All in all, single calendar and cycling models were built just considering the accelerated ageing time frame within which the induced degradation modes seemed to have kept the same. Once the degradation mechanisms are checked thoroughly and ratified by post-portem analysis, cell performance loss and degradation modes are to be simulated jointly over time. This way, model parameterisation step will be optimised and the predictions will be more reliable for the whole considered cell lifetime. Furthermore, due to the fact that the accelerated ageing tests are still ongoing, the presented cycling ageing model was developed using experimental data at different cell degradation rates. The aim was to at least estimate roughly and take into account single and combined effects of the studied factors. Hence, it cannot be left behind that these approximations enhance significantly the model error, since data at very short ageing periods were used (e.g. 2C & 60% DOD as well as 3.5C & 10% DOD tests) and 0.8 root of time capacity loss dependency was observed when DOD effect was just evaluated. It means that the different effects were not equally quantified and thus the used fitting introduces large prediction errors at intermediate cycling amplitudes (an error of *ca.* 4% was reached for 60% DOD test. See Fig. 7). Different modelling errors are depicted in Fig. 11, which shows the predictions goodness when: (i) just considering a single impact factor using either experimental data after different testing time periods (sections *b* and *f* in Fig. 11), (ii) matching new data with the model built beforehand (section *c* in Fig. 11), and (iii) even considering single and combined effects of multiple stress factors using data at different testing time periods (section *d+e+f* in Fig. 11). It is this way needless to say that it is worth running the cycling tests until there is available significantly large amount of assessable data (compare sections *c* and *f* in Fig. 11) and even better until the defined EOL is reached in the case of cyclic ageing so that different effects can be simulated as accurate as possible taking into account the different degradation modes to the extent possible.

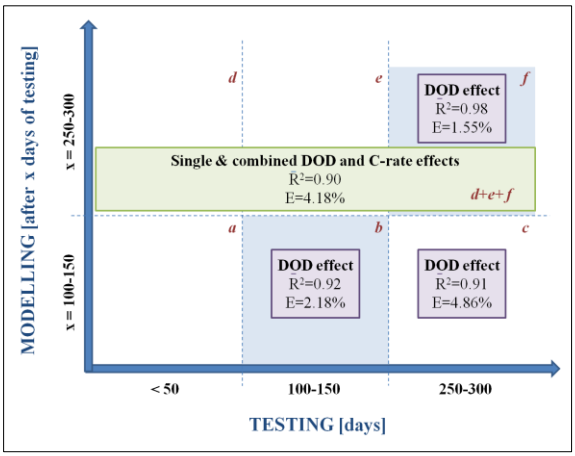

Figure 11: Cyclic ageing model precision and trustworthiness taking into account different amount of experimental data over time

3.2 Model validation

Fig. 12 represents both static and dynamic accelerated calendar and cyclic ageing tests (Fig. 3) results with the corresponding models prediction according to Eq. (5) and Eq. (6), respectively. The method used for predicting the capacity loss at dynamic profiles took into account the ageing by former usage. This way, the residual capacity was used as reference point for further predictions at different operating parameters and not simply the operating time [20][21].

The validation tests are still ongoing but, at first glance, the built calendar and cycling single models apparently are able to forecast the capacity loss due to dynamic operating conditions with a maximum error of 0.9% and 1.2%, respectively (Fig. 12). The results of the additional cycling test at static conditions (30% DOD, 1C) showed

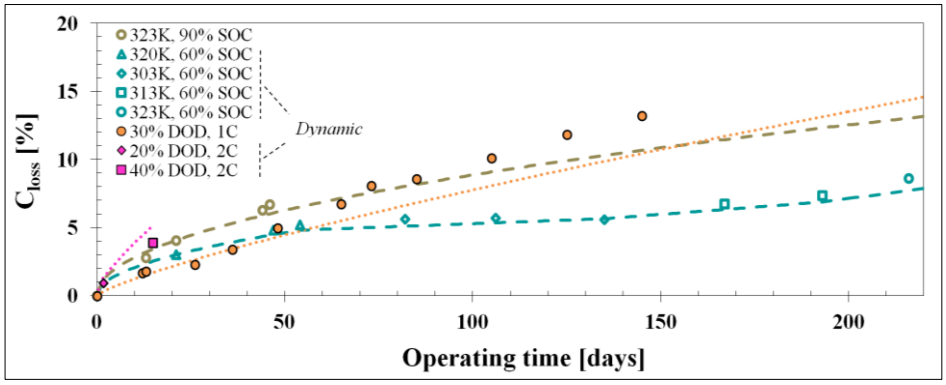

Figure 12: Calendar-life and cycle-life models static and dynamic verifications

$$C_{loss}=[165400\cdot exp(-4148/T)\cdot exp(0.01\cdot SOC)-B]\cdot t^{0.5}+[(-0.14-0.08\cdot DOD+1.92\cdot DOD^{0.5}-2.51\cdot ln(DOD))\cdot(0.48\cdot Crate^2-2.42\cdot Crate+1.57)]\cdot t^{0.8} \quad (7)$$

that the fittings at intermediate cycling amplitudes do not quantify *ca.* 2.8% of the measured capacity loss after 150 days of cycling, which highlights, as explained in the previous section, that more data is required for different impact factors parameterisation. On the contrary, the calendar ageing model follows the trend observed at new ageing static conditions (maximum assessed error of 0.7%), which once again ratified that induced degradation modes during storage are stable over time within the studied impact factors' level ranges. Anyway, for completing calendar ageing model verification, it is also to be evaluated the effect of aleatory SOC impact factor.

Last step in the methodology for lifetime prognosis (Fig. 1) is the superimposition of all the effects of the different stress factors quantified separately during either cycling or standing operation and the evaluation of this latter combined model adaptability to arbitrary conditions. Fig. 13 shows the results obtained randomly performing a profile defined within the considered studied stress factors' ranges (Fig. 3) and the corresponding predictions according to the model mathematically described in Eq. (7). Note that *B* factor in Eq. (7) corresponds to the capacity loss due to cell standing at 303K and 50%SOC during cycling (all the single cycling tests were carried out at these conditions). Hence, the value for *B* will be 0.290 in case the cell is working. Otherwise, if the cell is just stored, *B* will not exist in Eq. (7).

Maximum combined model's predictive error was 1.5%. The evaluated experimental results did not correspond to extended operating times, which ought to be carefully checked since the error is accumulative over time (it increased steadily from 0.5% to 1.5% in 21 days).

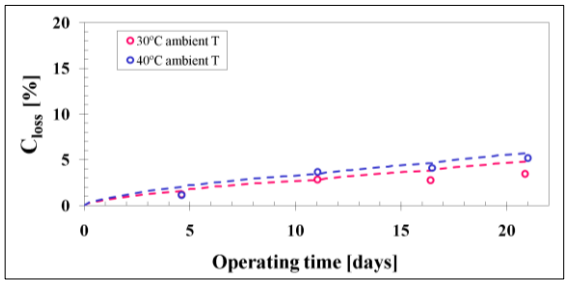

Figure 13: Model total validation. Dynamic DOD, C-rate, standing SOC, cell operating T and storing periods (outlined in Fig. 3) over time

Dynamic validation of IR model is also required. Due to the fact that it was concluded that the main stressing factor in this case is the temperature, IR evolution ought to have been checked at different storing temperatures. Unfortunately, the obtained experimental results were not relevant, as even after 193 days of storing between 303 and 323K the cell's IR was not increased (on the contrary, it was reduced).

3.3 Model applicability

Lifetime estimation algorithm could be potentially integrated in a BMS for SOH estimations. The developed ageing evaluation methodology enables deriving the SOH by monitoring either capacity or IR. The relevance of measuring and implementing these two ageing metrics depends on the target final application. For the specific cell configuration studied in this paper (LFP/graphite 26650-size cell), the IR increase over time was not significant, so SOH estimation would be accomplished by just measuring the capacity fade. Nevertheless, evaluating accurately IR evolution gather importance in case it is pursued to implement it in a thermal model. The aim in this latter case would be determining the cooling system that could help: (i) controlling and slowing

down the degradation rate due to cell heating, and (ii) operating within the cell safe operating temperature window, preventing this way thermal failure to the extent possible.

When it comes to the reliability of SOH predictions in a BMS, the estimations would be optimised in case other complementary techniques for measuring actual operating capacity were used. For instance, as shown in Fig. 14, were the model updated systematically, the margin of error would be reduced from 1.5 to 0.6% after 21 days of operation at realistic conditions (validation test shown in Fig. 13). Hence, using a predictor/corrector framework based on on-board measurements, battery operating and control strategies could be adjusted guaranteeing reliable battery prognosis.

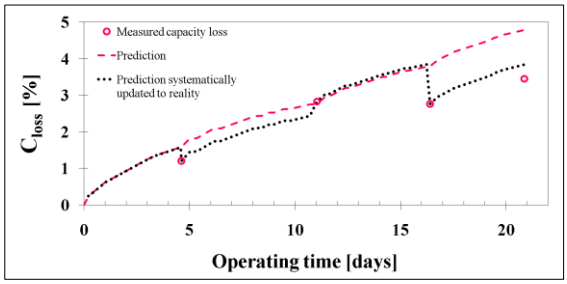

Figure 14: Capacity loss over time due to dynamic operating profile (outlined in Fig. 3), corresponding model prediction (Eq. (7)) and prediction corrected to the actual measured SOH

Implementing the ageing model into simulating tools, as shown in Fig. 4, makes possible evaluating performance losses due to different operating conditions and thus determining the best operating ranges for the studied stress factors depending on the pursued goal (longest lifespan, reduction of costs, enhancement of safety and so on). In this sense, at the same time, in depth analysis of DOD influence on the total either number of cycles or Ah-throughput that a cell can provide over the whole lifetime can serve, for instance, as clue guideline for battery pack sizing. Fig. 15 shows the total Ah-throughput estimations (until 20% capacity loss EOL is reached) as a function of cycling DOD calculated using the built cycling model (Eq. (6)). For the studied cell case, the total Ah-throughput does not strongly depend on the cycling amplitude but for very small DOD (5%), so it is key reaching the compromise of minimising costs due to either getting a larger small amount of energy or reducing the battery pack size to a tenth within the similar total energy output range. All the more, it might be of interest to reduce the battery pack size to even a twentieth if it is taken into account, on the one hand, that cell materials and depreciation costs respectively mean 27% and 16% of the total cost of an EV battery pack [22] and, on the other hand, that 10 years of lifetime are required for EV applications.

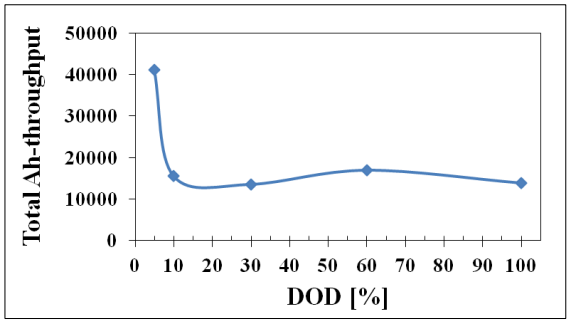

Figure 15: Estimations (according to Eq. (6)) of DOD dependant (cycling at 1C, mean 50% SOC and 30ºC) cell Ah-throughput during the defined whole lifetime. Make note that all the predictions were corrected according to the largest errors that were measured for each specific condition.

4 Conclusions

- It is feasible to build accurate ageing predictive models that simulate realistic operating profiles based on single cycling and calendar models. That is to say, storage and cyclic ageing effects can be apparently superimposed.
- Calendar ageing seems to be stable over time. Hence, defining the End of Test (EOT) will be a trade-off solution between the experimental costs to cover and predictions precision required by the end user.

  However, cyclic ageing is tedious to predict: it is required impact factors effects combinations and over time induced degradation modes in depth analysis.
- Static validations determine the precision of single impact factors parameterisation and provide useful guidelines for optimising or widening, if necessary, planned ageing test matrix.

  Dynamic validations, on the other hand, inform of the goodness of the predictions at aleatory operating conditions using models based on the evaluation of static impact factors. Not only do they strengthen the reliability and value of the predictions, but also enable sparing with time consuming and expensive ageing tests for models development.

- Diagnostics at dynamic conditions need to have into account the actualised SOH at all times, so monitoring the operating profile and updating the ageing model is a must in order that it can be implemented in a BMS.
- The developed lifetime predictive model is useful for battery pack sizing within beforehand evaluable (using the same model) wide range of operating conditions.

Acknowledgments

This work was supported by Emaitek and Etortek programmes of the Basque Government.

References

[1] H. Wenzl et al., *Life prediction of batteries for selecting the technically most suitable and cost effective battery*, Journal of Power Sources, 144 (2005), 373-384.

[2] E. V. Thomas et al., *Rate-based degradation modeling of lithium-ion cells*, Journal of Power Sources, 206 (2012), 378-382.

[3] M. Ecker et al., *Development of a lifetime prediction model for lithium-ion batteries based on extended accelerated aging test data*, Journal of Power Sources, 215 (2012), 248-257.

[4] K. J. Chung, C. C. Hsiao, *Accelerated Degradation Assessment of 18650 Lithium-ion Batteries*, 2012 International Symposium on Computer, Consumer and Control.

[5] E.V. Thomas, I. Bloom, *Statistical methodology for predicting the life of lithium-ion cells via accelerated degradation testing*, Journal of Power Sources, 184 (2008), 312-317.

[6] S. Käbitz et al., *Cycle and calendar life study of a graphite$LiNi_{1/3}Mn_{1/3}Co_{1/3}O_2$ Li-ion high energy system. Part A: Full cell characterization*, Journal of Power Sources (2013).

[7] F. Herb, *Alterungsmechanismen in Lithium-Ionen-Batterien und PEM-Brennstoffzellen und deren Einfluss auf die Eigenschaften von daraus bestehenden Hybrid-Systemen*, Dissertation zur Erlangung des Doktorgrades Dr. rer. nat. der Fakultät für Naturwissenschaften der Universität Ulm (2010).

[8] F. Herb et al. (Daimler), *Investigation of Li-battery and fuel cell aging in FC hybrid car model*, Eleventh Grove Fuel Cell Symposium, 23.Sep.2009, London.

[9] C. Günther et al. (ZSW), *Lifetime Models for Lithium-ion Batteries*, 2nd Technical Conference "Advanced Battery Technologies for Automobiles and Their Electric Power Grid Integration", 1-2 Feb. 2010, Rheingoldhalle, Mainz.

[10] W. Prochazka et al., *Design-of-Experiment and Statistical Modeling of a Large Scale Aging Experiment for Two Popular Lithium Ion* Cell *Chemistries*, ECS 160 (8) A1039-A1051 (2013).

[11] M. Dubarry et al., *Synthesize battery degradation modes via a diagnostic and prognostic model*, Journal of Power Sources 2019 (2012) 201-216.

[12] P. Liu et al., *Aging Mechanisms of $LiFePO_4$ Batteries Deduced by Electrochemical and Structural Analyses*, Journal of Electrochemical Society, 157 (2010), A499-A507.

[13] M. Safari and C. Delacourt, *Aging of a Commercial Graphite/$LiFePO_4$ Cell*, Journal of Electrochemical Society 158 (2011) A1123-A1135.

[14] J. Groot, *State-of-Health Estimation of Li-ion Batteries: Cycle Life Test Methods*, Thesis for the degree of Licentiate of Engineering, Division of Electric Power Engineering, Department of Energy and Environment. Göteborg, Sweden, Chalmers University of Technology.

[15] F. Herb. et al., *Optimization of fuel cell and battery control in relation to component aging of fuel cell power train*, At-Automatisierungstechnik, 57 (2009), 40-47.

[16] R. Arunachala, *Depelopment of an Aging Model for Lithium Ion Batteries based on Calendar Aging Tests*, Master Thesis-RWTH Aachen University (2011).

[17] H.J. Ploehn et al., *Solvent Diffusion Model for Aging of Lithium-Ion Battery Cells*, *Journal of The Electrochemical Society*, 151 (3) A456-A462 (2004).

[18] J. Wang et al., *Cycle-life model for graphite-LiFePO4 cells*, Journal of Power Sources, 196 (2011), 3942-3948.

[19] E. Scott et al., *A practical Longevity Model for Lithium-Ion Batteries: De-coupling the Time and Cycle-Dependence of Capacity Fade*, 208th ECS Meeting (2005).

[20] H. Wenzl et al., *Degradation of Lithium Ion Batteries under Complex Conditions of Use*, Z. Phys. Chem. 227 (2013) 57-74.

[21] M. Leopiorz et al. (Siemens), *Ah-throughput versus residual capacity method for prediction of capacity loss of Li-ion batteries at alternating temperatures*, Advanced Battery Power 2013, Aachen, Germany.

[22] *Cost and performance of EV batteries*, Final report for The Committee on Climate Change. Element Energy Limited, 2012.

Authors

M.Eng. Elixabet Sarasketa Zabala received her M.Eng. degree in Chemical Engineering from the Faculty of Engineering of Bilbao (ETSI de Bilbao) and Master in Energy Systems from the University of Gävle (HIG, Sweden) in 2009, and Master in Information and Communication Technologies from the Faculty of Engineering of Mondragon University in 2012. She is a Ph.D. student at the Energy Business Unit of IK4-Ikerlan since 2009. She worked as visiting researcher at the Institute for Power Electronics and Electrical Drives (ISEA) of RWTH Aachen in the Electrochemical Conversion and Storage Systems Group during July-Dec. 2012.

M.Sc. Izaro Laresgoiti received her Physics degree from The Complutense University of Madrid and Master in Nanosciences from The University of the Basque Country in 2009. From 2010 to 2011 she worked on Li-ion battery degradation and modeling at the Institute for Power Electronics and Electrical Drives (ISEA) of RWTH Aachen in the Electrochemical Conversion and Storage Systems Group. She joined IK4-Ikerlan in 2011 as researcher within Electrical Energy Storage Team.

Dr. Chem. Isabel Alava received her MSc on Chemistry in 1992 and PhD degree in 1996 from The University of the Basque Country. She joined IK4-Ikerlan in 1997 and has more than 15 years experience working on Thermal and Combustion Processes. Since 2010, she works in the Electrical Energy Storage Research Team.

M.Eng. Mikel Rivas Gutiérrez received his M.Eng. in Chemical Engineering from The University of the Basque Country in 2004, with Master's thesis project in NTNU-Norwegian University of Science and Technology. He joined IK4-Ikerlan in 2004 and was involved in SOFC projects until 2009. Since 2010 he works in the Electrical Energy Storage Research Team.

Dr. Chem. Igor Villarreal received the M.Sc. on Chemistry from UNIZAR in 1996 and a PhD in Lithium ion Batteries in 2001 from CSIC-UCM of Madrid. He joined IK4-Ikerlan in 2000. He was working in LBNL between 2001 and 2003 as a visiting researcher. Since 2010 he is an Area Manager at IK4-Ikerlan and joined the Electrical Energy Storage Research Team. He is the coordinator of European Project Batteries 2020.

Dr. Eng. Francisco Blanco received the M.Sc. degree on Physics from Universidad Autónoma de Madrid in 1998 and a M.Eng (2000) and PhD in Electrical Engineering (2006) from Technical University of Madrid. He held several Engineering, R&D and Management positions in companies of the ICT and Energy Sectors (Acciona Energy, BP, Lucent Technologies and Philips). Currently, he is the IK4-Ikerlan Energy Business Director and also the head of the Electrical Energy Storage Research Team.